Research Article

# Intelligent control of induction motor for photovoltaic water pumping system

Mustapha Errouha[1] · Saad Motahhir[2] · Quentin Combe[3] · Aziz Derouich[1]

Received: 12 March 2021 / Accepted: 4 August 2021
Published online: 19 August 2021


**Abstract**
This work aims to improve the performance of direct torque control (DTC) technique for induction motor based photovoltaic (PV) water pumping system (PVWPS). The innovative aspect of this work consists in introducing the adaptive fuzzy logic control and the fuzzy logic control techniques as alternative approaches to conventional DTC to control the PVWPS. To ensure a good operation of the PV array, a variable step size incremental conductance (VSS INC) is implemented. Simulation studies of the proposed topology based on intelligent approaches will be investigated using Matlab/Simulink under various operating conditions to validate the suitability of the proposed PVWPS. From the obtained results, the proposed control strategies appear to be very convenient for water pumping applications.

**Article Highlights**

- An intelligent control based on the advanced techniques is proposed for PV water pumping system.
- An adaptive fuzzy logic PID approach and optimal fuzzy rules are proposed for better operation of PV system.
- The suggested PV water pumping system achieves better performance, in particular minimization of torque and flux ripples, reduction of torque overshoot and high dynamic response.

**Keywords** Photovoltaic water pumping system · Adaptive fuzzy logic control · Fuzzy logic control · Variable step size incremental conductance · Direct torque control

## 1 Introduction

Different water pumping systems use the electricity and diesel to run the pump. However, this kind of source has several drawbacks such as environmental pollution, low reliability, fossil fuel prices, low efficiency and high maintenance costs [1,2, 3]. Therefore, it is necessary to use a sustainable and appropriate alternative source to power the water pumping systems. The use of the renewable energy sources is the best solution to overcome the aforementioned drawbacks. Various renewable energy technologies such as solar, wind and biomass energies can be used for water pumping [4]. The solar photovoltaic technology is the most desired and suitable one because it is clean, naturally available and without noise [5].

As the output characteristics of the PV array are influenced by the meteorological conditions and the maximum efficiency is assured by one operating point, it's necessary to introduce MPPT algorithms to function in maximum power point (MPP) under different irradiation levels. A

✉ Saad Motahhir, saad.motahhir@usmba.ac.ma | [1]Laboratory of Industrial Technologies and Services, Higher School of Technology, SMBA University, Fez, Morocco. [2]Engineering, Systems and Applications Laboratory, ENSA, SMBA University, 30000 Fez, Morocco. [3]LEMTA, University of Lorraine, Vandœuvre-lès-Nancy, France.

variety of MPPT algorithms have been designed. Each algorithm has its own limitations, applications and specifications [6]. Perturb and observe and incremental conductance methods are the most used. Incremental conductance (INC) techniques provide good performance for most of the solar tracking applications [7]. The proposed PV water pumping system utilizes INC algorithm based on variable step size for better PV power optimization under fast changing atmospheric conditions [8].

Different types of motors are utilized for solar fed water pumping system with water pump. In [9], the authors use the synchronous reluctance motor. In [10], the authors introduce the induction motors [8]. Other researchers employ the permanent magnet synchronous motor to drive the pump [11]. In the PV water pumping applications, the induction motor provides better performance as compared to other commercial engines because it is a rugged machine, widely used in industries, cost effective and low cost [12].

However, the control of this type of motor is complex because of the nonlinear model. the scalar control technique is used to control the IM due to its lower cost and complexity but it offers unsatisfactory torque response on low frequencies [13]. In [14, 15], the authors propose the indirect field oriented control method. This technique provides good precision of speed and a satisfactory torque response on the full speed range. However, this control strategy depends on machine parameters. To achieve better control of the system, direct torque control (DTC) technique is introduced [16, 17].

This method offers better performance than scalar control and indirect field oriented control methods because it is simple to implement, less dependent on IM parameters and doesn't require current regulation loops. Also, DTC has a fast response [18, 19]. However, the presence of the hysteresis controller generates large flux and torque ripples [20]. On the one hand, this is a result of using a fixed width of the hysteresis bands. Moreover, the use small values of bandwidths keeps the presence of ripples and increases inverter switching frequency, and on the other hand to the utilization of switching vector for complete sample time period. The insertion of fuzzy logic controller replaces the hysteresis controllers and preserves a constant switching frequency which allows to reduce the high flux and torque ripples. To overcome these drawbacks, the multilevel converter is utilized in [21, 22], however, this method increases the cost and the losses. Other researchers have proposed the space vector modulation to improve the performance of the conventional DTC [23], however, the flux and torque loop PI regulators need an accurate design. The intelligent techniques are also employed by many researchers to enhance the controller performances. In [24], the artificial neural network is utilized, but this technique requires powerful calculation processes and is very complex. Fuzzy logic controller ensures good performance, especially, for the complex system where the mathematical model does not exist or is severely nonlinear [25]. The behavior of a physical variable is represented by membership functions which are selected in a way that they describe the real behavior of the variable. The choice of the kind of membership functions depends on the application and the designer's knowledge and experience, which are defined based on the experience of control systems. Sigmoidal, singleton, triangular, gaussian, trapezoidal and bell-shaped membership functions are Frequently employed. The triangular membership function turns out the most used and suitable membership function to control electric motors [26]. In [19], the hysteresis controllers and the look-up table are replaced by fuzzy logic blocks by keeping the conventional PI controller for speed regulation. As results, the flux and torque ripples are minimized. Although the advantages of the fuzzy logic controller, it can get more high performance by associating other techniques to drive the system. In [27], the authors propose an approach associated to fuzzy logic controller to select the optimal flux and variable step size Perturb and observe technique to extract the maximum power. This technique allows to reduce the losses and improve the efficiency. Moreover, the classical proportional-integral (PI) controller is used for speed regulation.

In [28], variable step size incremental conductance based maximum power tracking (MPPT) algorithm is utilized to control the duty ratio of DC-DC converter. The control of induction motor is achieved through fuzzy logic control based on direct torque method. However, the classical PI controller is adopted for speed regulation.

The conventional PI controller is the most widely employed for speed regulation due to its simple design and control structure. However, this controller provides larger overshoot, oscillation, lower response and the control performance is influenced by the external load disturbances and the variations of the parameters [29].

Moreover, the operating of the PV water pumping system using an optimal speed controller allows to start earlier, increase the pumped water and achieve a longer run time. In [30], the authors propose a genetic algorithm (GA) optimized PI and fuzzy sliding mode speed control for DTC technique. DTC using fuzzy-PI controllers is proposed in [31]. An improved Direct Torque Control using PI controller tuned using genetic algorithm is introduced in [32]. Therefore, an adaptive fuzzy controller for speed regulation is proposed in this paper to ensure optimal control performance during dynamic and steady state conditions.

However, to the authors' best knowledge, the combining of adaptive fuzzy controller for the speed regulation and fuzzy logic DTC for a PV water pumping system has

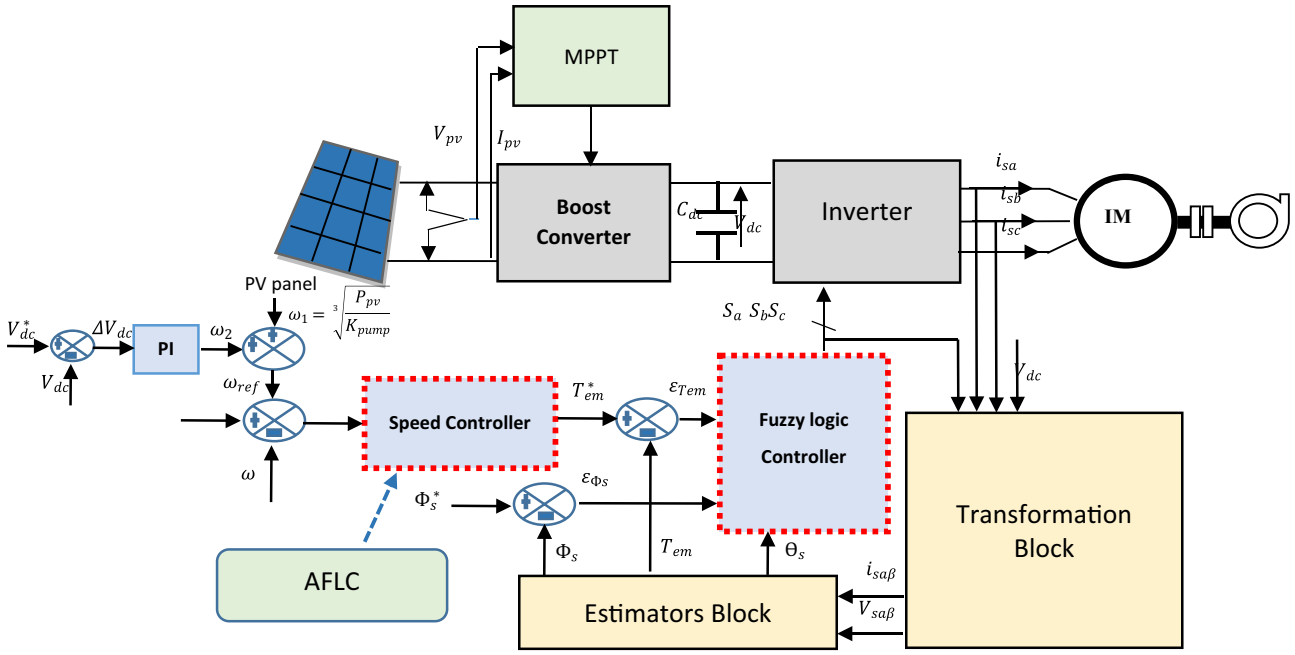


**Fig. 1** Proposed PV water pumping system

never been discussed. This allows us to propose a PV water pumping system based on the combining of the smart regulators (AFLC and FLC) for the first time in the literature.

Simulation studies of the proposed topology based on intelligent approaches will be investigated using Matlab/Simulink under various operating conditions to validate the suitability of the proposed PVWPS. Therefore, the use of intelligent techniques to control the PV water system provides better performance. The rest of the paper is organized as follows: the proposed system is designed in Sect. 2. Section 3 presents the conventional method. Section 4 describes the proposed control strategies. The results and discussion are given in Sect. 5. Finally, Sect. 6 provides the conclusions of this work and suggestions for future work.

## 2 Modeling of proposed PV system

The proposed PV water pumping system consists of an IM of 1,5 kW power rating and PV array of 1.88 kW peak power capacity under standard test conditions (Fig. 1) The characteristics of Csun235-60p PV panel and the used IM are listed in Tables 1 and 2 respectively.

### 2.1 PV panel

Different types of PV panels are made to respond to the needs and demands of the users. To assure the necessary energy, the PV panels are associated in series or parallel.

**Table 1** Characteristics of PV panel

| Maximum Power, Pmax | 235 W |
|---|---|
| Open Circuit Voltage, Voc | 36.8 V |
| Short Circuit Current, Isc | 8.59 A |
| Maximum Power Voltage Pmax,Vmpp | 29.5 V |
| Maximum Power Current Pmax, Impp | 7.97 A |
| Standard Test Condition (STC) | 1000 W/m$^2$, 25 °C, AM 1.5 |

**Table 2** Motor parameters

| Stator resistance $R_s$ & inductance $l_s$ | 1.8 [Ω] & 0.104 [H] |
|---|---|
| Rotor resistance $R_r$ & inductance $l_r$ | 2.227[Ω] & 0.104 [H] |
| Inertia J | 0.0588[Kg.m$^2$] |
| Mutual inductance M | 0.0959 [H] |
| Number of pole pairs p | 4 |
| Viscous Friction $f_v$ | 0.1352 [N.m.s/rad] |

The equivalent circuit of the utilized PV panel is illustrated in Fig. 2 [7, 33, 34]

The current produced by the PV panel can be expressed by:

$$I = I_{ph} - I_0\left(\exp\frac{q(V+RI)}{aKTN_S} - 1\right) - \frac{(V+IR)}{R_{sh}} \quad (1)$$

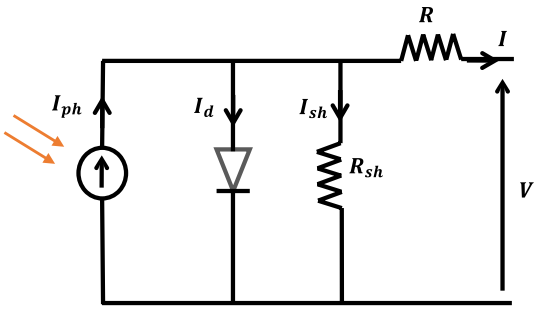


**Fig. 2** PV panel equivalent circuit

#### 2.1.1 Boost converter

This type of converter has a simple structure (Fig. 3). Moreover, it's characterized by higher efficiency of conversion. The outputs current and voltage of the converter can be written as follows [35]:

$$V_{dc} = \frac{V_{pv}}{1-\alpha} \tag{2}$$

$$I_{dc} = I_{pv}(1-\alpha) \tag{3}$$

The parameters of the of boost converter are calculated as follows:

| Component | Expression | Used value |
|---|---|---|
| $C_{dc}$ | $C_{dc}=\frac{6\alpha V_{LL} It}{[V_{dc}^{*2}-V_{dc}^2]}$ | 2000 µF |
| α | $\alpha=\frac{V_{dc}-V_{mp}}{V_{dc}}$ | 0.26 |
| $L_{pv}$ | $L_{pv}=\frac{DV_{mp}}{\Delta I f_s}$ | 3 mH |

where
$V_{dc}^*$: Estimated DC voltage
$C_{dc}$: DC link capacitor
$V_{dc}$: Selected DC voltage
$I$: Phase current motor

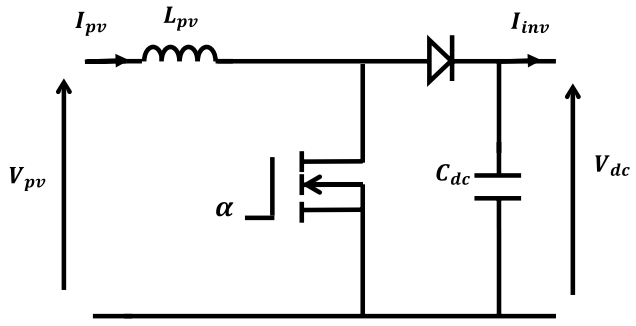


**Fig. 3** Boost converter

$V_{LL}$: Phase voltage motor.
$t$: Duration of transient
$D$: Overloading factor
$L_{pv}$: Inductance of the Boost converter
$\Delta I$: Amount of ripple content current
$f_s$: Frequency of switching,
α: Duty cycle.

### 2.2 Two level inverter

The inverter is introduced to ensure the DC/AC conversion and control the speed of the motor. It's composed of 6 Insulated Gate Bipolar Transistors. The outputs voltages of the inverter in terms of Vdc can be written as follows [36]

$$V_a = \frac{V_{dc}}{3}(2S_a - S_{b-}S_c) \tag{4}$$

$$V_b = \frac{V_{dc}}{3}(-S_a + 2S_{b-}S_c) \tag{5}$$

$$V_c = \frac{V_{dc}}{3}(-S_a - S_b + 2S_c) \tag{6}$$

where: $S_a, S_b, S_c$: logic control signals.

### 2.3 Induction motor

Based on the simplifying assumptions, the mathematical model of the induction machine can be expressed by the following equations [25]:

$$\begin{cases} \frac{d\phi_{\alpha s}}{dt} = V_{\alpha s} - R_s i_{\alpha s} \\ \frac{di_{\alpha s}}{dt} = -\left(\frac{R_s}{\sigma l_s} - \frac{R_r}{\sigma l_r}\right) i_{\alpha s} - w_r i_{\beta s} + \frac{R_r}{\sigma l_r l_s}\phi_{\alpha s} + \frac{w_r}{\sigma l_s}\phi_{\beta s} + \frac{1}{\sigma l_s}V_{\alpha s} \\ \frac{d\phi_{\beta s}}{dt} = V_{\beta s} - R_r i_{\beta s} \\ \frac{di_{\beta s}}{dt} = -\left(\frac{R_s}{\sigma l_s} - \frac{R_r}{\sigma l_r}\right) i_{\beta s} - w_r i_{\alpha s} + \frac{R_r}{\sigma l_r l_s}\phi_{\beta s} - \frac{w_r}{\sigma l_s}\phi_{\alpha s} + \frac{1}{\sigma l_s}V_{\beta s} \end{cases} \tag{7}$$

where
$R_s, R_r$: Stator and rotor resistances
$i_{\alpha s}, i_{\beta s}$: Stator current components
$l_s, l_r$ : Stator and rotor inductances
$\phi_{\alpha s}, \phi_{\beta s}$: Stator flux components
$\sigma$: leakage factor.
The expression of the electromagnetic torque $T_{em}$ can be written as follows:

$$T_{em} = \frac{3}{2}P(\phi_{\alpha s} i_{\beta s} - \phi_{\beta s} i_{\alpha s}) \tag{8}$$

### 2.4 Centrifugal pump

The load torque of the pump $T_{pump}$ can be expressed in terms of the proportionality constant $K_{pump}$ and the rotational speed as follows [37, 38]:

$$T_{pump} = K_{pump} w^2 \tag{9}$$

## 3 Direct torque control strategy

To control the IM driven water pumping system, DTC method is introduced. It's considered one of the most utilized ones. This classical technique uses the hysteresis controllers to control the stator flux and the torque. The two-level hysteresis controller is used for the stator flux in which the input is the flux error resulting from the comparison between the referential and estimated values while the output is a Boolean variable that determines the increase or the decrease in the flux. However, the three-level hysteresis controller is used for the torque to define the increase or the decrsease in the torque. The Boolean variables and the stator flux vector position allow to determine the adequate inverter state to attain an appropriate torque from the switching table (Table 3). Moreover, the reference torque is obtained from the PI speed controller. The correctors keep the torque and flux within defined limits [39, 40].

Based on the model of the IM, the stator flux vector can be expressed as follows [41]:

$$\overrightarrow{\Phi_s}(t) = \int_0^t (\overrightarrow{V_S}(t) - R_s \vec{i_s}(t))dt \tag{10}$$

The magnitude and components of stator flux $\Phi_{s\alpha}$ and $\Phi_{s\beta}$ are estimated as follows [42]:

$$\Phi_{s\alpha}(t) = \int_0^t (V_{s\alpha}(t) - R_s i_{s\alpha}(t))dt \tag{11}$$

$$\Phi_{s\beta}(t) = \int_0^t (V_{s\beta}(t) - R_s i_{s\beta}(t))dt \tag{12}$$

$$\Phi_s = \sqrt{\Phi_{s\alpha}^2 + \Phi_{s\beta}^2} \tag{13}$$

Moreover, the estimated electromagnetic torque can be expressed by:

$$T_{em} = \frac{3}{2} P(\Phi_{s\alpha} i_{s\beta} - \Phi_{s\beta} i_{s\alpha}) \tag{14}$$

In addition, the phase angle of the stator flux can be written as follows:

$$\Phi_s = \tan^{-1}\left(\frac{\Phi_{s\beta}}{\Phi_{s\alpha}}\right) \tag{15}$$

## 4 Speed PI controller synthesis

The PV water pumping system functions at variable speed which requires the use of speed controller for producing the reference torque (Fig. 4). The speed reference is determined by two components. The first one is obtained from DC link voltage controller as mentioned above. The second component is calculated by [37]:

$$\omega_1 = \sqrt[3]{\frac{P_{pv}}{K_{pump}}} \tag{16}$$

The reference speed can be expressed by:

$$\omega_{ref} = \omega_1 + \omega_2 \tag{17}$$

The parameters of the speed controller are:
$K_p$= 5.7, $K_i$= 240.

## 5 DC-link voltage controller

The proportional-integral (PI) controller is introduced to maintain the DC bus voltage constant at its reference value (Fig. 5). Moreover, the second component of the reference

**Table 3** Switching Table

| Sector | 1 | 2 | 3 | 4 | 5 | 6 |
|---|---|---|---|---|---|---|
| $\varepsilon_{\Phi s} = 0$ | $\varepsilon_{Tem} = 1$ V3 | V4 | V5 | V6 | V1 | V2 |
| | $\varepsilon_{Tem} = 0$ V0 | V7 | V0 | V7 | V0 | V7 |
| | $\varepsilon_{Tem}$ =-1 V5 | V6 | V1 | V2 | V3 | V4 |
| $\varepsilon_{\Phi s} = 1$ | $\varepsilon_{Tem} = 1$ V2 | V3 | V4 | V5 | V6 | V1 |
| | $\varepsilon_{Tem} = 0$ V7 | V0 | V7 | V0 | V7 | V0 |
| | $\varepsilon_{Tem}$ =–1 V6 | V1 | V2 | V3 | V4 | V5 |

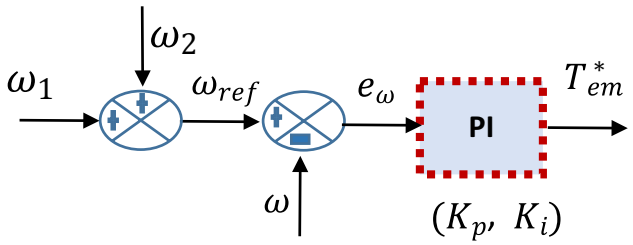


**Fig. 4** Speed controller

speed ($\omega_2$) is obtained from this controller. The voltage error ($\Delta V_{dc}$) which results from the comparison between the reference bus voltage and the measured bus voltage ($V_{dc}$) can be expressed as follows [43]:

$$\Delta V_{dc} = V^*_{dc} - V_{dc} \tag{18}$$

The output of the DC link voltage PI controller is expressed by:

$$\omega_1 = \omega_{1(K-1)} + K_{pdc}\left\{\Delta V_{dc(k)} - \Delta V_{dc(k-1)}\right\} + K_{idc}\Delta V_{dc(k)} \tag{19}$$

The parameters of DC-link voltage controller are: $K_{pdc} = 0.4$, $K_{idc} = 1.7$

## 6 Variable step size incremental conductance

Due to the low conversion efficiency of PV panel, the maximum power point tracking MPPT algorithm must be introduced to extract the maximum possible power from the PV array. Among the developed algorithms, the incremental conductance technique is often employed because of its high performance in terms of efficiency and tracking speed. It's based on the power variation by calculating the incremental conductance and the conductance. The derivative of PV power by the voltage is zero means that the maximum power point is achieved. The equation of this algorithm can be expressed by:

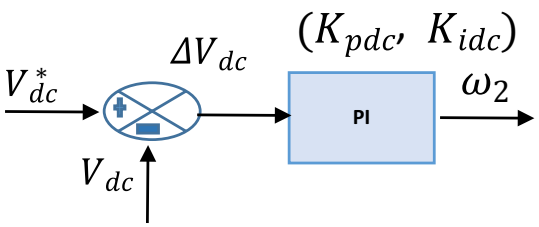


**Fig. 5** DC link voltage controller

$$\frac{dP_{pv}}{dV_{pv}} = \frac{d(V_{pv}I_{pv})}{dV_{pv}} = I_{pv} + V_{pv}\frac{dI_{pv}}{dV_{pv}} = 0 \tag{20}$$

However, the conventional incremental conductance technique uses a fixed step size to track the power which reduces the performance under rapidly changing atmospheric conditions. Therefore, The incremental conductance based on variable step size is introduced to track MPP using the derivative of the Ppv with respect Vpv and assure good functioning under rapidly changing atmospheric conditions (Fig. 6) [28]:

## 7 Proposed control strategies

The proposed control scheme of the PV water pumping system is composed of two steps: the first one consists of replacing the switching table by fuzzy logic controller while the second step consists of introducing the adaptive fuzzy logic controller for speed regulation.

### 7.1 Adaptive fuzzy logic controller

The bloc of the adaptive fuzzy logic controller consists of three principal steps (Fig. 7): fuzzification, bloc inference and defuzzification [44]. The inputs of the controller are speed error $e_\omega$(k) and change of speed error $\Delta e_\omega$ while the outputs are $\Delta K_i$ and $\Delta K_p$ which allow to adapt the integral gain $K_i$ and proportional gain $K_p$.

In the fuzzification step, based on the appropriate gains values, the inputs and outputs normalized in the interval [−1, 1] and fuzzified using the following linguistic variables (Fig. 8):

- NB is negative big;
- PB is positive big.
- NM is negative middle;
- PM is positive middle
- NS is negative small;
- PS is positive small;
- ZO is zero;

Tables 4 and 5 resume the adaptive FLC fuzzy rules:

The fuzzy inference is achieved using the Mamdani's Min–Max technique. The degree of membership for $\Delta K_p$ and $\Delta K_i$ can be determined as follows:

$$\mu_D(\Delta K_p) = \bigvee_{j=1}^{49}\left\{\left[\mu_{Aj}(e_\omega)\ \Lambda\mu_{Bj}(\Delta e_\omega)\right]\Lambda\mu_{Dj}(\Delta K_p)\right\} \tag{21}$$

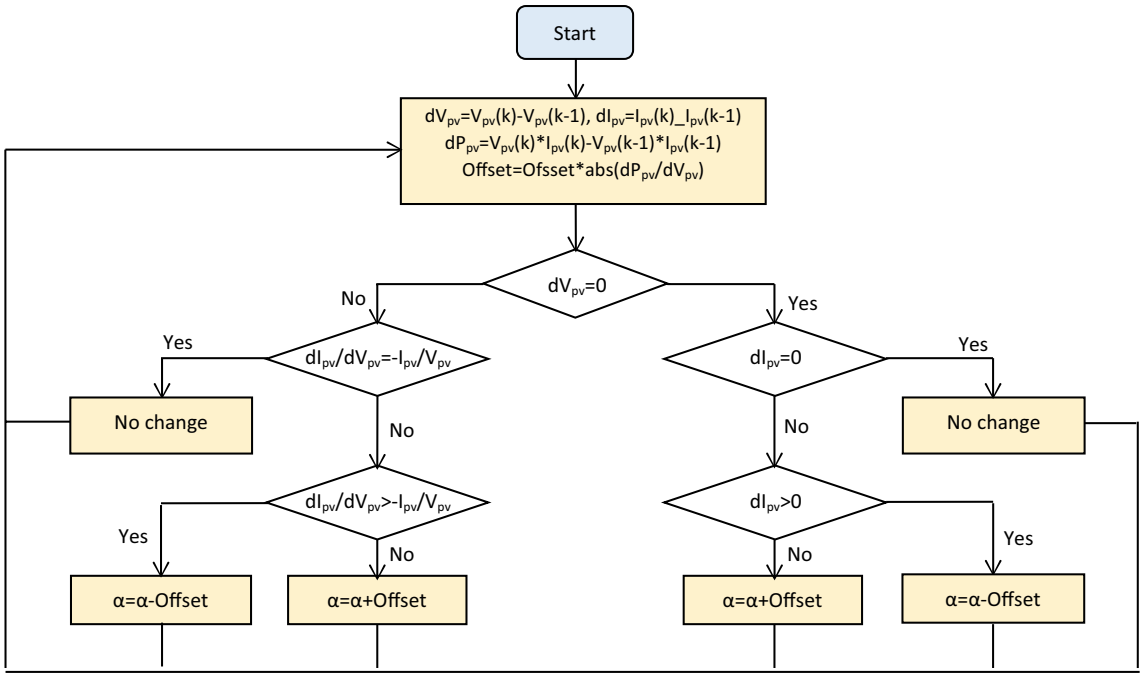


**Fig. 6** MPPT algorithm

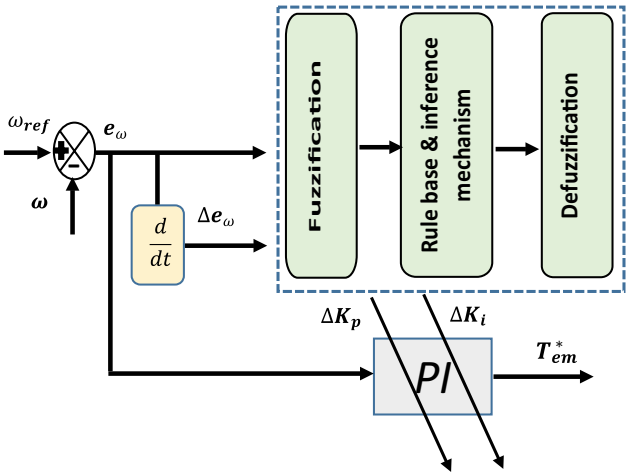


**Fig. 7** Structure of AFLC

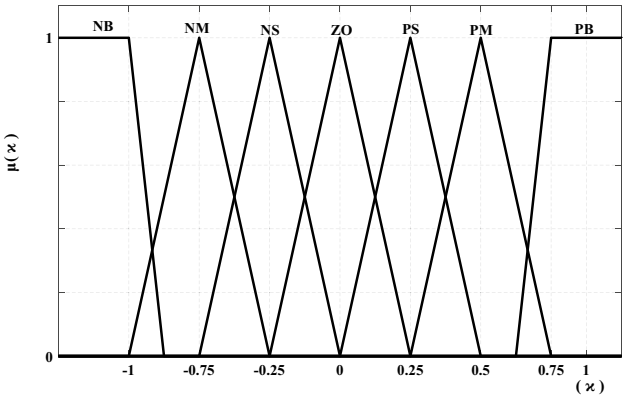


**Fig. 8** Membership functions

$$\mu_{\sigma}(\Delta K_p) = \bigvee_{j=1}^{49} \{[\mu_{Aj}(e_{\omega}) \wedge \mu_{Bj}(\Delta e_{\omega})] \wedge \mu_{\sigma j}(\Delta K_p)\} \quad (22)$$

In the defuzzification step, the center of gravity technique is adopted to convert fuzzy variables to crisp values. Therefore, $\Delta K_p$ and $\Delta K_i$ can be determined by the following equations:

$$\Delta K_p(e_{\omega}, \Delta e_{\omega}) = \frac{\sum_{j=1}^{49} P_{Oj}\mu_{\sigma j}(\Delta K_p)}{\sum_{j=1}^{49} \mu_{\sigma j}(\Delta K_p)} \quad (23)$$

$$\Delta K_i(e_{\omega}, \Delta e_{\omega}) = \frac{\sum_{j=1}^{49} I_{Oj}\mu_{\sigma j}(\Delta K_i)}{\sum_{j=1}^{49} \mu_{\sigma j}(\Delta K_i)} \quad (24)$$

Therefore, we obtain:

$$\begin{cases} K_p = K_p(0) + \Delta K_p \\ K_i = K_i(0) + \Delta K_i \end{cases} \quad (25)$$

where: $K_p(0)$, $K_i(0)$: the initial parameters.

### 7.2 Fuzzy logic controller

In order to get more high performance, the fuzzy logic controller is introduced.

#### 7.2.1 Fuzzification

Triangular and singleton MFs are utilized for the inputs and outputs respectively. The linguistic variables employed for membership functions are: negative (N) and positive (P) and zero (Z) for the flux error (Fig. 9a), negative large (NL), positive large (PL), negative small (NS), zero (Z) and positive small (PS) for the torque error (Fig. 9b), $\theta_1$ to $\theta_{12}$ for the sector angle determination (Fig. 9c) and "0", "1" for the converter's switches $S_i$ (Fig. 9d).

#### 7.2.2 Fuzzy rules

In this step, a suitable rule-base based on the input and the outputs must be elaborated. Therefore, it can be defined as follows:

**Table 4** $\Delta K_p$ fuzzy rules

| | | $\Delta e(k)$ | | | | | | |
|---|---|---|---|---|---|---|---|---|
| | | PB | PM | PS | ZO | NS | NM | NB |
| $e(k)$ | NB | ZO | ZO | PS | PM | PM | PB | PB |
| | NM | NS | ZO | PS | PS | PM | PB | PB |
| | NS | NS | ZO | PS | PS | PM | PM | PM |
| | ZO | NM | NM | NS | ZO | PS | PM | PM |
| | PS | NM | NM | NS | NS | ZO | PS | PS |
| | PM | NB | NM | NM | NM | NS | ZO | PS |
| | PB | NB | NB | NM | NM | NM | ZO | ZO |

**Table 5** $\Delta K_i$ fuzzy rules

| | | $\Delta e(k)$ | | | | | | |
|---|---|---|---|---|---|---|---|---|
| | | PB | PM | PS | ZO | NS | NM | NB |
| $e(k)$ | NB | ZO | ZO | NS | NM | NM | NB | NB |
| | NM | ZO | ZO | NS | NS | NM | NB | NB |
| | NS | PS | PS | ZO | NS | NS | NM | NB |
| | ZO | PM | PM | PS | ZO | NS | NM | NM |
| | PS | PB | PM | PS | PS | ZO | NS | NM |
| | PM | PB | PB | PM | PS | PS | ZO | ZO |
| | PB | PB | PB | PM | PM | PS | ZO | ZO |

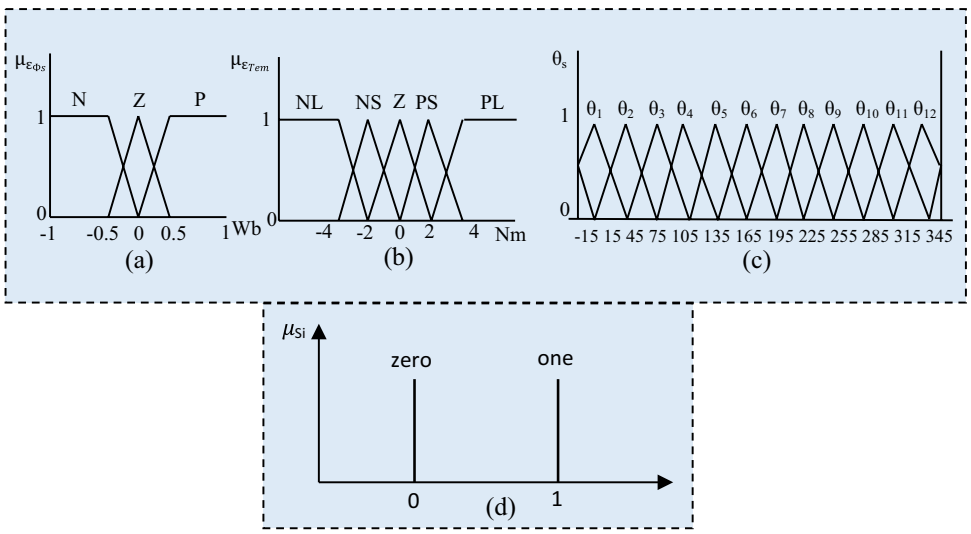


**Fig. 9** Membership functions of input and output variables

IF($\varepsilon_{\Phi_s}$ is $A_{N,Z,P}$) AND ($\varepsilon_{T_{em}}$ is $B_{NL,NS,Z,PS,PL}$) AND ( $\theta_s$ is $\theta_{s1,12}$) THEN ($S_a$ is $D_{0,1}$) AND ($S_b$ is $D_{0,1}$) AND ($S_c$ is $D_{0,1}$).

where

$A_{N,Z,P}$, $B_{NL,NS,Z,PS,PL}$, $\theta_{s1,12}$: the inputs fuzzy sets.

$D_{0,1}$: the outputs fuzzy sets.

The fuzzy inference system inputs contain three, five and twelve fuzzy sets respectively which involve a set of one hundred eighty rules (3 * 5 * 12). Thus, Table 6 illustrates the inference matrix which represents the rules.

#### 7.2.3 Defuzzification

This step consists of elaborating the switches 'state which are obtained from the output of the fuzzy controller. Therefore, the max method is introduced and expressed by the following equation:

$$\mu\text{Vout}'(\text{V}) = \max_{i=1}^{180}\max(\mu\text{Vout}'(\text{V})) \quad (26)$$

where:

$\mu$Vout′: membership degree.

## 8 Results and discussion

The response of the suggested PV water pumping system is analyzed with the help of simulations carried out in MATLAB/Simulink. Different modes of operation are analyzed under various solar insolation levels to evaluate the dynamic response of the PV system. A comparative study of the proposed PV system based on intelligence artificial techniques with the PV system based on the conventional DTC (C_DTC) is effectuated.

### 8.1 Starting state performances of PV the system

Figure 10a and b illustrate the solar radiation profile and the extracted PV power using MPPT algorithm for the insolation of 1000 W/m$^2$ respectively. Figure 10c shows the extracted PV power without MPPT technique. It can be seen that the power reaches the maximun power (1880 W) while the power of the PV panel reaches 275 W without MPPT algorithm. Figure 10d and e show the rotor speed and the pumped water for both techniques. Using the proposed technique, the speed response is faster compared to conventional DTC. In addition, a speed overshoot appears and its value equal to 2% when the PV system is controlled by the classical technique.

Figure 10f shows the electromagnetic torque provided by the IM controlled by the proposed technique and C_ DTC. It's clear that the torque overshoot of the conventional method is higher than this with artificial intelligence techniques. It reaches 15.5 Nm while the torque overshoot of the proposed techniques reaches 14.6 Nm. In addition, a high starting torque degrades the performance of the system. On the other hand, a significant reduction of torque ripples is obtained by using the proposed technique which leads to improve the performance and the efficiency of the PV water pumping system.

Figure 10g illustrates the response of the developed stator flux for both control strategies.it can be noticed that the proposed method based on artificial intelligence techniques provides less flux ripples.

Figure 10h and i show the trajectory of stator flux alpha and beta for the proposed method and C_DTC. In Fig. 10h, it can be observed that big oscillations are produced. From Fig. 10i, the aforementioned ripples and

**Table 6** Fuzzy rules

| $\varepsilon_{(Tem)}$ | $\varepsilon_{(\varphi s)}$ | $\Theta_s$ | | | | | | | | | | | |
|---|---|---|---|---|---|---|---|---|---|---|---|---|---|
| | | $\theta_1$ | $\theta_2$ | $\theta_3$ | $\theta_4$ | $\theta_5$ | $\theta_6$ | $\theta_7$ | $\theta_8$ | $\theta_9$ | $\theta_{10}$ | $\theta_{11}$ | $\theta_{12}$ |
| PL | Z | $V_2$ | $V_3$ | $V_3$ | $V_4$ | $V_4$ | $V_5$ | $V_5$ | $V_6$ | $V_6$ | $V_1$ | $V_1$ | $V_2$ |
| PS | | $V_2$ | $V_3$ | $V_3$ | $V_4$ | $V_4$ | $V_5$ | $V_5$ | $V_6$ | $V_6$ | $V_1$ | $V_1$ | $V_2$ |
| Z | | $V_7$ | $V_0$ | $V_7$ | $V_0$ | $V_7$ | $V_0$ | $V_7$ | $V_0$ | $V_7$ | $V_0$ | $V_7$ | $V_0$ |
| NS | | $V_7$ | $V_0$ | $V_7$ | $V_0$ | $V_7$ | $V_0$ | $V_7$ | $V_0$ | $V_7$ | $V_0$ | $V_7$ | $V_0$ |
| NL | | $V_6$ | $V_1$ | $V_1$ | $V_2$ | $V_2$ | $V_3$ | $V_3$ | $V_4$ | $V_4$ | $V_5$ | $V_5$ | $V_6$ |
| PL | N | $V_3$ | $V_4$ | $V_4$ | $V_5$ | $V_5$ | $V_6$ | $V_6$ | $V_1$ | $V_1$ | $V_2$ | $V_2$ | $V_3$ |
| PS | | $V_4$ | $V_4$ | $V_5$ | $V_5$ | $V_6$ | $V_6$ | $V_1$ | $V_1$ | $V_2$ | $V_2$ | $V_3$ | $V_3$ |
| Z | | $V_7$ | $V_0$ | $V_7$ | $V_0$ | $V_7$ | $V_0$ | $V_7$ | $V_0$ | $V_7$ | $V_0$ | $V_7$ | $V_0$ |
| NS | | $V_5$ | $V_5$ | $V_6$ | $V_6$ | $V_1$ | $V_1$ | $V_2$ | $V_2$ | $V_3$ | $V_3$ | $V_4$ | $V_4$ |
| NL | | $V_5$ | $V_6$ | $V_6$ | $V_1$ | $V_1$ | $V_2$ | $V_2$ | $V_3$ | $V_3$ | $V_4$ | $V_4$ | $V_5$ |
| PL | P | $V_2$ | $V_3$ | $V_3$ | $V_4$ | $V_4$ | $V_5$ | $V_5$ | $V_6$ | $V_6$ | $V_1$ | $V_1$ | $V_2$ |
| PS | | $V_2$ | $V_2$ | $V_3$ | $V_3$ | $V_4$ | $V_4$ | $V_5$ | $V_5$ | $V_6$ | $V_6$ | $V_1$ | $V_1$ |
| Z | | $V_0$ | $V_7$ | $V_0$ | $V_7$ | $V_0$ | $V_7$ | $V_0$ | $V_7$ | $V_0$ | $V_7$ | $V_0$ | $V_7$ |
| NS | | $V_1$ | $V_1$ | $V_2$ | $V_2$ | $V_3$ | $V_3$ | $V_4$ | $V_4$ | $V_5$ | $V_5$ | $V_6$ | $V_6$ |
| NL | | $V_6$ | $V_1$ | $V_1$ | $V_2$ | $V_2$ | $V_3$ | $V_3$ | $V_4$ | $V_4$ | $V_5$ | $V_5$ | $V_6$ |

**Fig. 10** Performance of PV system under starting state

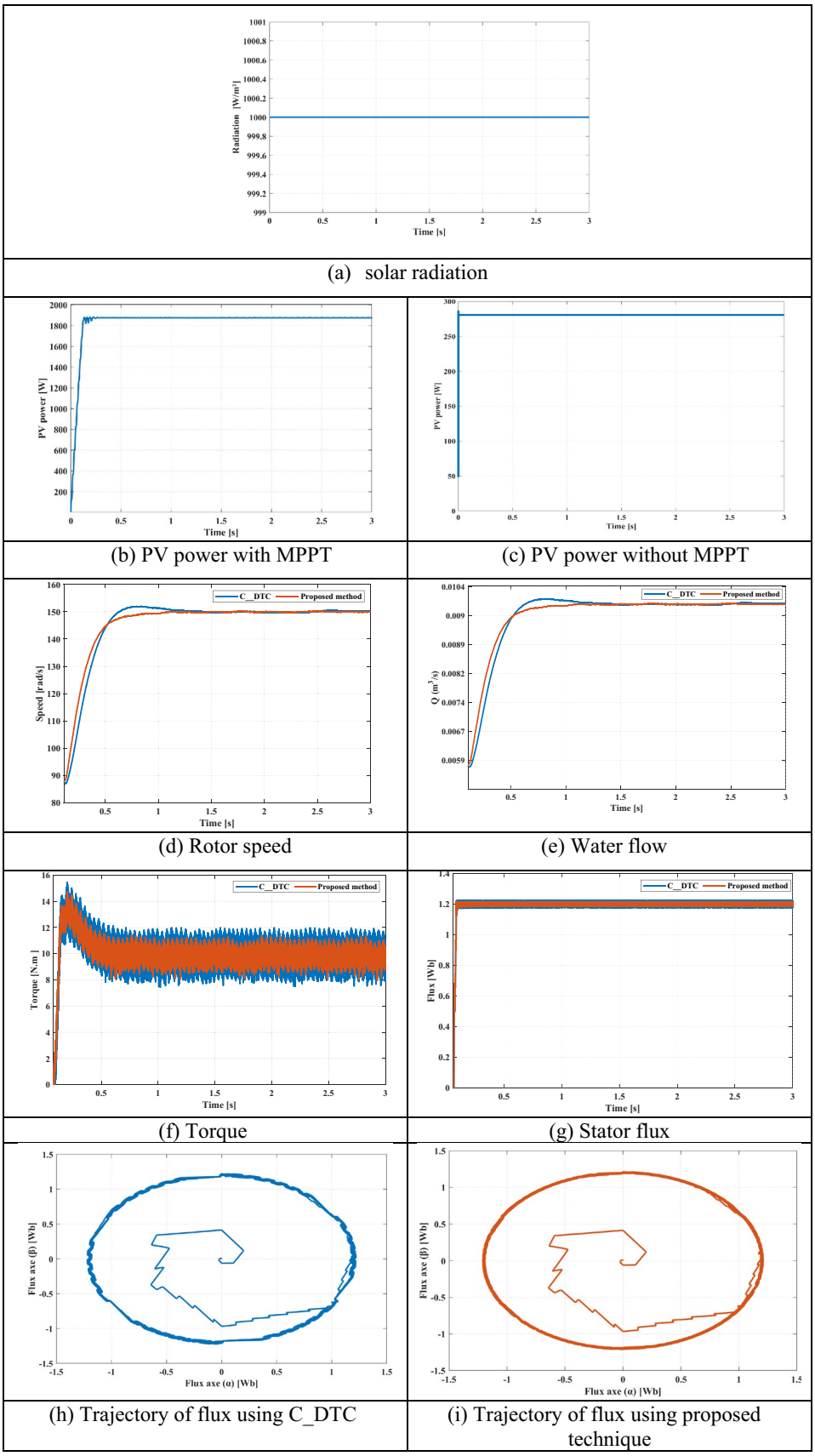

oscillations are reduced. Moreover, we obtain a perfect circular trajectory using the proposed method.

### 8.2 Sudden change of solar irradiance

A sudden change of solar irradiance is applied to PV water pumping from the solar insolation of 1000 W/m$^2$ to 500 W/m$^2$ at 3 s (Fig. 11a). Figure 11b and c illustrate the obtained PV power using VSS INC and without MPPT technique. We can notice that the maximum power is extracted from the PV panel using VSS INC for all solar irradiance levels.

Figure 11d and e show the rotor speed and the pumped water for both techniques. The response of rotor speed obtained using the proposed method takes 0.9 s to reach the reference while the C_DTC technique takes 1.5 s. As consequence, the improvement of the response time is clear.

Figure 11f illustrates the developed electromagnetic torque of IM using both methods. At the change of the solar irradiance, the torque ripples of the PV water pumping system controlled by the proposed technique are minimized. Contrary to the PV system controlled by the C_DTC, the oscillations of the torque are higher.

Figure 11g shows the developed stator flux of the IM issued by C_DTC and the proposed method. It can be seen that the flux ripples based on artificial intelligence techniques are minimized during the simulation period.

Figure 11h and i show the trajectory of stator flux alpha and beta for the proposed method and C_DTC under sudden change of solar irradiance. From Fig . 11h, it can be observed high oscillations on stator flux using the C_DTC method. However, we observe that stator flux controlled by the proposed method assures perfect circular trajectory.

Table 7 resumes the main improvements of the proposed method based on artificial intelligence techniques compared to C_DTC.

From the presented data, the proposed method based on the combination of AFLC and FLC provides better performance in terms of reduction of overshoot, ripples and the improvement of response time.

A performance comparison of the proposed control strategy and other techniques used for PV water pumping system is summarized in Table 8. We mention that they do not refer to the same conditions because it is very difficult to find several studies effectuated under the same conditions. Hence, a comparison based on the response time, torque ripples and rise time is carried out. Therefore, the proposed PV water pumping system provides better performance.

## 9 Conclusion

A solar PV water pumping system based on the combination of artificial intelligence techniques is presented. The proposed control consists of introducing the fuzzy logic controller to give the suitable switching keys to function the centrifugal pump and the adaptive fuzzy logic control for speed regulation. In addition, variable step size INC is introduced to ensure better operation of the proposed system. A comparative study between the proposed and conventional methods are investigated to prove the robustness of the proposed PV water pumping system. Under these comparisons, the suggested control strategies are more efficient and more likely to be utilized in PV water pumping applications compared to C_DTC. We can notice that the major improvements of this work are:

- Minimization of flux and torque ripples
- The increasing of pumped water flow
- Reduction of overshoot and undershoot
- Enhancement of the response time

The next stage of our research will be the experimental validation of the proposed control strategies. Besides, other artificial intelligence techniques will be proposed for PV water pumping applications.

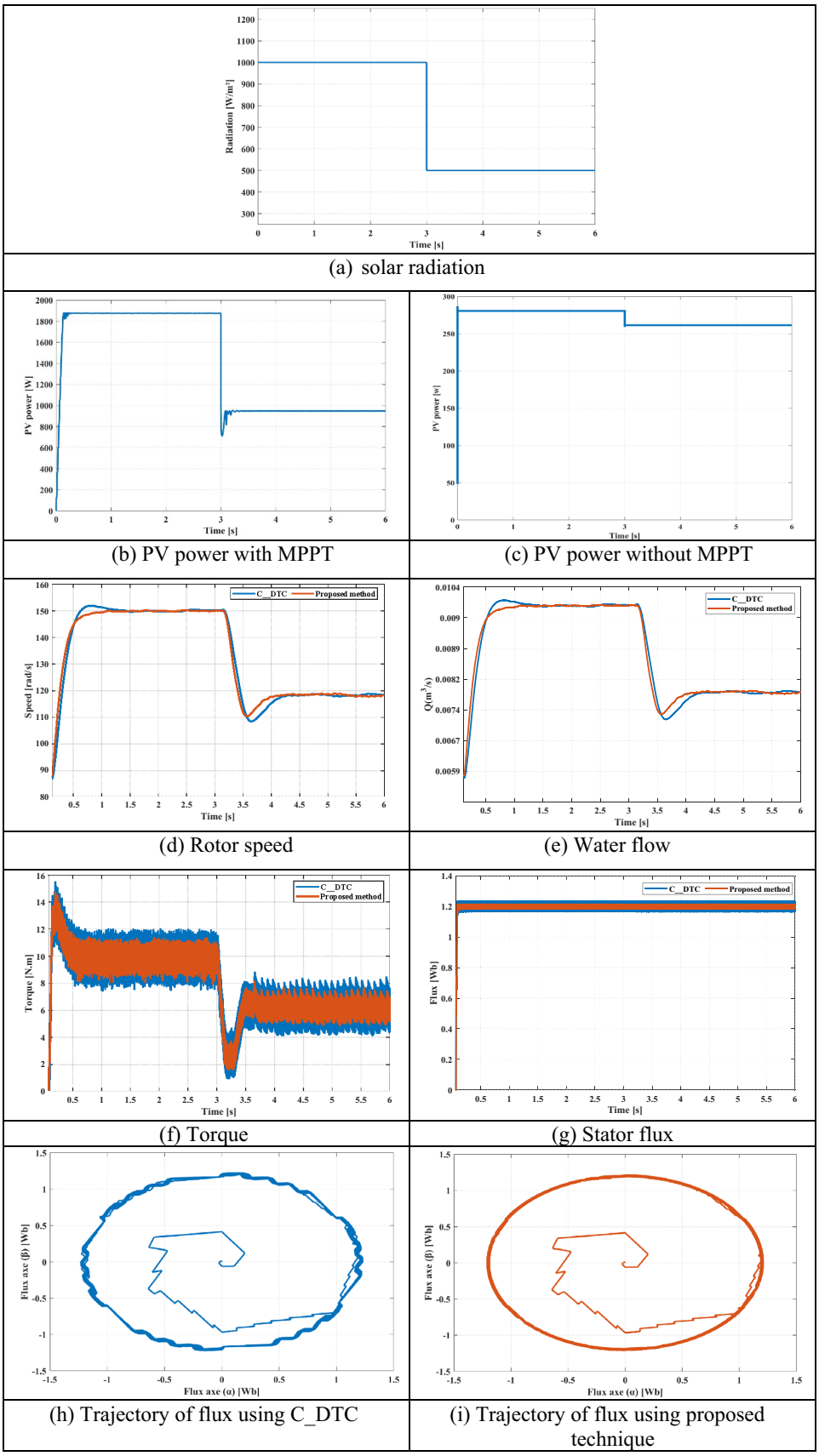


(a) solar radiation

(b) PV power with MPPT

(c) PV power without MPPT

(d) Rotor speed

(e) Water flow

(f) Torque

(g) Stator flux

(h) Trajectory of flux using C_DTC

(i) Trajectory of flux using proposed technique

**Fig. 11** Performance of PV system under variable insolation

**Table 7** Performance of PV system

| Operating mode | | Starting state | | Sudden change of solar radiance | |
|---|---|---|---|---|---|
| Performance | C_DTC | Proposed_DTC | C_DTC | Proposed_DTC | Proposed_DTC |
| Speed | Overshoot (%) | 2 | 0 | – | – |
| | Response time (s) | 0.8 | 0.45 | 3.93 | 3.5 |
| | Undershoot (%) | – | – | 8 | 6 |
| Torque | Ripple (N.m) | 4.364 | 2.46 | 4.575 | 2.408 |
| Flux | Ripple (Wb) | 0.06 | 0.02 | 0.069 | 0.021 |

**Table 8** Comparison between the proposed technique and other methods used for PVWPS

| Publications | Response time (s) | Torque ripples (N.m) | Rise time (s) |
|---|---|---|---|
| [45] | 0.9 | 4.3 | 0.7 |
| [46] | 0.8 | 4.1 | 0.58 |
| [47] | 0.5 | 4 | 0.4 |
| Proposed technique | 0.45 | 2.46 | 0.37 |

## Declarations

**Conflict of interest** On behalf of all authors, the corresponding author states that there is no conflict of interest.



## References

1. Liu B, Wang Z, Feng L, Jermsittiparsert K (2021) Optimal operation of photovoltaic/diesel generator/pumped water reservoir power system using modified manta ray optimization. J Clean Prod 289:125733. https://doi.org/10.1016/j.jclepro.2020.125733
2. Errouha M, Derouich A, Nahid-Mobarakeh B, Motahhir S, El Ghzizal A (2019) Improvement control of photovoltaic based water pumping system without energy storage. Sol Energy 190:319–328. https://doi.org/10.1016/j.solener.2019.08.024
3. El Hammoumi A, Motahhir S, Chalh A, El Ghzizal A, Derouich A (2018) Real-time virtual instrumentation of Arduino and LabVIEW based PV panel characteristics. IOP Conf Ser Earth Environ Sci. https://doi.org/10.1088/1755-1315/161/1/012019
4. Gopal C, Mohanraj M, Chandramohan P, Chandrasekar P (2013) Renewable energy source water pumping systems - a literature review. Renew Sustain Energy Rev 25:351–370. https://doi.org/10.1016/j.rser.2013.04.012
5. Meunier S et al (2019) A validated model of a photovoltaic water pumping system for off-grid rural communities. Appl Energy 241:580–591. https://doi.org/10.1016/j.apenergy.2019.03.035
6. Karami N, Moubayed N, Outbib R (2016) General review and classification of different MPPT Techniques. Renew Sustain Energy Re 68(1–18):2017
7. Muhsen DH, Khatib T, Nagi F (2017) A review of photovoltaic water pumping system designing methods, control strategies and field performance. Renew Sustain Energy Rev 68:70–86
8. Loukriz A, Haddadi M, Messalti S (2016) Simulation and experimental design of a new advanced variable step size incremental conductance MPPT algorithm for PV systems. ISA Trans 62:30–38. https://doi.org/10.1016/j.isatra.2015.08.006
9. Zaky AA et al (2020) Energy efficiency improvement of water pumping system using synchronous reluctance motor fed by perovskite solar cells. Int J Energy Res 44(14):11629–11642. https://doi.org/10.1002/er.5788
10. Ben Ammar R, Ben Ammar M, Oualha A (2020) Photovoltaic power forecast using empirical models and artificial intelligence approaches for water pumping systems. Renew Energy 153:1016–1028. https://doi.org/10.1016/j.renene.2020.02.065
11. Prabhakaran KK, Karthikeyan A, Varsha S, Perumal BV, Mishra S (2020) Standalone single stage PV-Fed reduced switch inverter based PMSM for water pumping application. IEEE Trans Ind Appl 56(6):6526–6535. https://doi.org/10.1109/TIA.2020.3023870
12. Singh B, Sharma U, Kumar S (2018) Standalone photovoltaic water pumping system using induction motor drive with reduced sensors. IEEE Trans Ind Appl 54(4):3645–3655. https://doi.org/10.1109/TIA.2018.2825285
13. Ayman S, Neama Yussif AMM, Sabry OH, Abdel-Khalik AS (2021) Enhanced quadratic V/f-based induction motor control of solar water pumping system. Energies, 14
14. Yahyaoui I, Serna Cantero A (2018) Scalar and vector control of induction motor for online photovoltaic pumping, 1. Elsevier Inc.,
15. Errouha M, Nahid-mobarakeh B, Motahhir S, Combe Q, Derouich A (2021) Embedded Implementation of Improved IFOC for Solar Photovoltaic Water Pumping System Using dSpace. Green Energy Technol. https://link.springer.com/chapter/10.1007/978-3-030-64565-6_15
16. Moulay-Idriss C, Mohamed B (2013) Application of the DTC control in the photovoltaic pumping system. Energy Convers Manag 65:655–662. https://doi.org/10.1016/j.enconman.2011.08.026
17. Krim S, Gdaim S, Mtibaa A, Mimouni MF (2019) "Control with high performances based DTC strategy: FPGA implementation and experimental validation. EPE J (Eur Power Electron Drives J) 29(2):82–98
18. Tazerart F, Mokrani Z, Rekioua D, Rekioua T (2015) Direct torque control implementation with losses minimization

of induction motor for electric vehicle applications with high operating life of the battery. Int J Hydrogen Energy 40(39):13827–13838. https://doi.org/10.1016/j.ijhydene.2015.04.052
19. Gdaim S, Mtibaa A, Mimouni MF (2014) Design and experimental implementation of DTC of induction machine based on fuzzy logic control on FPGA. https://doi.org/10.1109/TFUZZ.2014.2321612.
20. Reza CMFS, Islam MD, Mekhilef S (2014) A review of reliable and energy efficient direct torque controlled induction motor drives. Renew Sustain Energy Rev 37:919–932. https://doi.org/10.1016/j.rser.2014.05.067
21. Ramulu C, Sanjeevikumar P, Karampuri R, Jain S, Ertas AH, Fedak V (2016) A solar PV water pumping solution using a three-level cascaded inverter connected induction motor drive. Eng Sci Technol an Int J 19(4):1731–1741. https://doi.org/10.1016/j.jestch.2016.08.019
22. Tarusan SAA, Jidin A, Jamil MLM (2021) The optimization of torque ripple reduction by using DTC-multilevel inverter. ISA Trans. https://doi.org/10.1016/j.isatra.2021.04.005
23. Krim S, Gdaim S, Mtibaa A, Mimouni MF (2016) FPGA contribution in photovoltaic pumping systems : models of MPPT and DTC-SVM algorithms, 6(3)
24. Khan K, Shukla S, Sing B (2018) Design and development of high efficiency induction motor for PV array fed water pumping. Proc 2018 IEEE Int Conf Power Electron Drives Energy Syst PEDES. pp. 1–6, doi: https://doi.org/10.1109/PEDES.2018.8707578
25. Sudheer H, Kodad SF, Sarvesh B (2017) Improvements in direct torque control of induction motor for wide range of speed operation using fuzzy logic. J Electr Syst Inf Technol. https://doi.org/10.1016/j.jesit.2016.12.015
26. Zangeneh M, Aghajari E, Forouzanfar M (2020) A survey: fuzzify parameters and membership function in electrical applications. Int J Dyn Control 8(3):1040–1051. https://doi.org/10.1007/s40435-020-00622-1
27. Errouha M, Derouich A, Motahhir S, Zamzoum O (2020) Optimal control of induction motor for photovoltaic water pumping system. Technol Econ Smart Grids Sustain Energy. https://doi.org/10.1007/s40866-020-0078-9
28. M. Errouha, A. Derouich, N. El Ouanjli, and S. Motahhir, "High-Performance Standalone Photovoltaic Water Pumping System Using Induction Motor," *Int. J. Photoenergy*, vol. 2020, 2020.
29. Terki A, Moussi A, Betka A, Terki N (2012) An improved efficiency of fuzzy logic control of PMBLDC for PV pumping system. Appl Math Model 36(3):934–944. https://doi.org/10.1016/j.apm.2011.07.042
30. Gadoue SM, Giaouris D, Finch JW (2007) Genetic algorithm optimized PI and fuzzy sliding mode speed control for DTC drives. Lect Notes Eng Comput Sci 2165(1):475–480
31. Rocha-Osorio CM, Solís-Chaves JS, Casella IRS, Capovilla CE, Azcue Puma JL, Sguarezi Filho AJ (2017) GPRS/EGPRS standards applied to DTC of a DFIG using fuzzy – PI controllers. Int J Electr Power Energy Syst 93:365–373. https://doi.org/10.1016/j.ijepes.2017.05.033
32. Zemmit A, Messalti S, Harrag A (2018) A new improved DTC of doubly fed induction machine using GA-based PI controller. Ain Shams Eng J 9(4):1877–1885. https://doi.org/10.1016/j.asej.2016.10.011
33. Motahhir et al (2020) Optimal energy harvesting from a multi-strings PV generator based on artificial bee colony algorithm. IEEE Syst J. https://doi.org/10.1109/jsyst.2020.2997744
34. Errouha E, Motahhir S, Combe Q, Derouich A (2021) Parameters extraction of single diode PV model and application in solar pumping. pp 178–191. https://doi.org/10.1007/978-3-030-62199-5_16
35. Sudipta Chakraborty MGS, Kramer WE (2014) Power electronics for renewable and distributed energy systems, 8(2)
36. Praveen Kumar KV, Kumar TV (2017) An effective four-level voltage switching state algorithm for direct torque controlled open end winding induction motor drive by using two two-level inverters. Electr Power Comp Syst 45(19):2175–2187
37. Murshid S, Singh B (2019) Implementation of PMSM drive for a solar water pumping system. IEEE Trans Ind Appl 55(5):4956–4964. https://doi.org/10.1109/TIA.2019.2924401
38. Errouha M, Derouich A, Motahhir S, Zamzoum O, El Ouanjli N, El Ghzizal A (2019) Optimization and control of water pumping PV systems using fuzzy logic controller. Energy Rep 5:853–865. https://doi.org/10.1016/j.egyr.2019.07.001
39. Jannati M et al (2017) A review on variable speed control techniques for efficient control of single-phase induction motors: evolution, classification, comparison. Renew Sustain Energy Rev 75:1306–1319. https://doi.org/10.1016/j.rser.2016.11.115
40. Krim S, Gdaim S, Mtiba A, Mimouni MF (2015) Fuzzy speed controller for an induction motor associated with the direct torque control: implementation on the FPGA. 2015 4th Int Conf Syst Control ICSC pp. 492–497. https://doi.org/10.1109/ICoSC.2015.7153297
41. Errouha M, Motahhir S, Combe Q, Derouich A, El Ghzizal A (2019) Fuzzy-PI Controller for Photovoltaic Water Pumping Systems. In 2019 7th International Renewable and Sustainable Energy Conference (IRSEC), Agadir, Morocco, Morocco
42. Krim S, Gdaim S, Mtibaa A, Mimouni MF (2015) Design and implementation of direct torque control based on an intelligent technique of induction motor on FPGA. J Electr Eng Technol 10(4):1528–1540. https://doi.org/10.5370/JEET.2015.10.4.1528
43. Arfaoui J, Rezk H, Al-Dhaifallah M, Ibrahim MN, Abdelkader M (2020) Simulation-based coyote optimization algorithm to determine gains of PI controller for enhancing the performance of solar PV water-pumping system. Energies. https://doi.org/10.3390/en13174473
44. Mesloub H, Benchouia MT, Boumaaraf R, Goléa A, Goléa N, Becherif M (2018) Design and implementation of DTC based on AFLC and PSO of a PMSM. Math Comput Simul. https://doi.org/10.1016/j.matcom.2018.04.010
45. Achour A, Rekioua D, Mohammedi A, Mokrani Z, Rekioua T, Bacha S (2016) Application of direct torque control to a photovoltaic pumping system with sliding-mode control optimization. Electr Power Comp Syst. https://doi.org/10.1080/15325008.2015.1102182
46. Abouda S, Nollet F, Chaari A, Essounbouli N, Koubaa Y (2013) Direct torque control - DTC of induction motor used for piloting a centrifugal pump supplied by a photovoltaic generator. Int J Electr Comput Eng 7(8):1110–1115. https://doi.org/10.5281/zenodo.1089096
47. Mirshekarpour B, Alireza Davari S (2016) Efficiency optimization and power management in a stand-Alone photovoltaic (PV) water pumping system, 7th Power Electron Drive Syst Technol Conf PEDSTC 2016, doi: https://doi.org/10.1109/PEDSTC.2016.7556899